Automatic Interferogram Selection for SBAS-InSAR Based on Deep Convolutional Neural Networks

Yufang He [1,2], Guangzong Zhang [1,*], Hermann Kaufmann [3] and Guochang Xu [1]

[1]Institute of Space Science and Applied Technology, Harbin Institute of Technology (Shenzhen), Shenzhen 518055, China;

[2]GFZ German Research Centre for Geosciences, Department of Geodesy, Section of Remote Sensing, Potsdam 14473,Germany;

[3]School of Space Science and Physics, Shandong University at Weihai, Weihai 264209, China.

EGU General Assembly 2022

NH6.1 – Remote sensing big data analysis and applications in geosciences

1 Background

Interferometric synthetic aperture radar

InSAR

- High spatial resolution, high efficiency
- Work day and night
- Large-scale surface deformation monitoring
- Millimeter-level monitoring accuracy

D_InSAR → **TS_InSAR** → **Geological Hazard Monitoring**

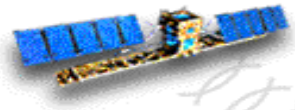

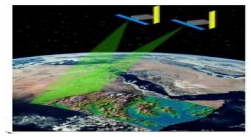

SAR

Classical Method

SBAS_InSAR

Small baseline subset (SBAS) InSAR:

- Parallel SBAS (P-SBAS)
- Multidimensional SBAS (M-SBAS)
- New SBAS (N-SBAS)
- Pixel-offset SBAS.

1 Background

The **key operation** for SBAS_InSAR : Selection of high-quality interferograms

Methods

- **The traditional manual method,** large amount of human-computer interaction;
- **The optimal temporal and spatial baseline thresholds method,** low-quality interferograms may be mistaken ;
- **Triangulation reduction and a simulated annealing (SA) searching strategy,** long time of operation;
- **The graph theory (GT),** not suitable for all SAR images with severe atmospheric distortions.

➢ **Don't meet requirements of automation and high efficiency engineering application for the big data era.** We need **automated and effective** method.

Deep Convolutional Neural Networks (**DCNN**) method → ResNet Model → ResNet50 Model

2 Methods and contents

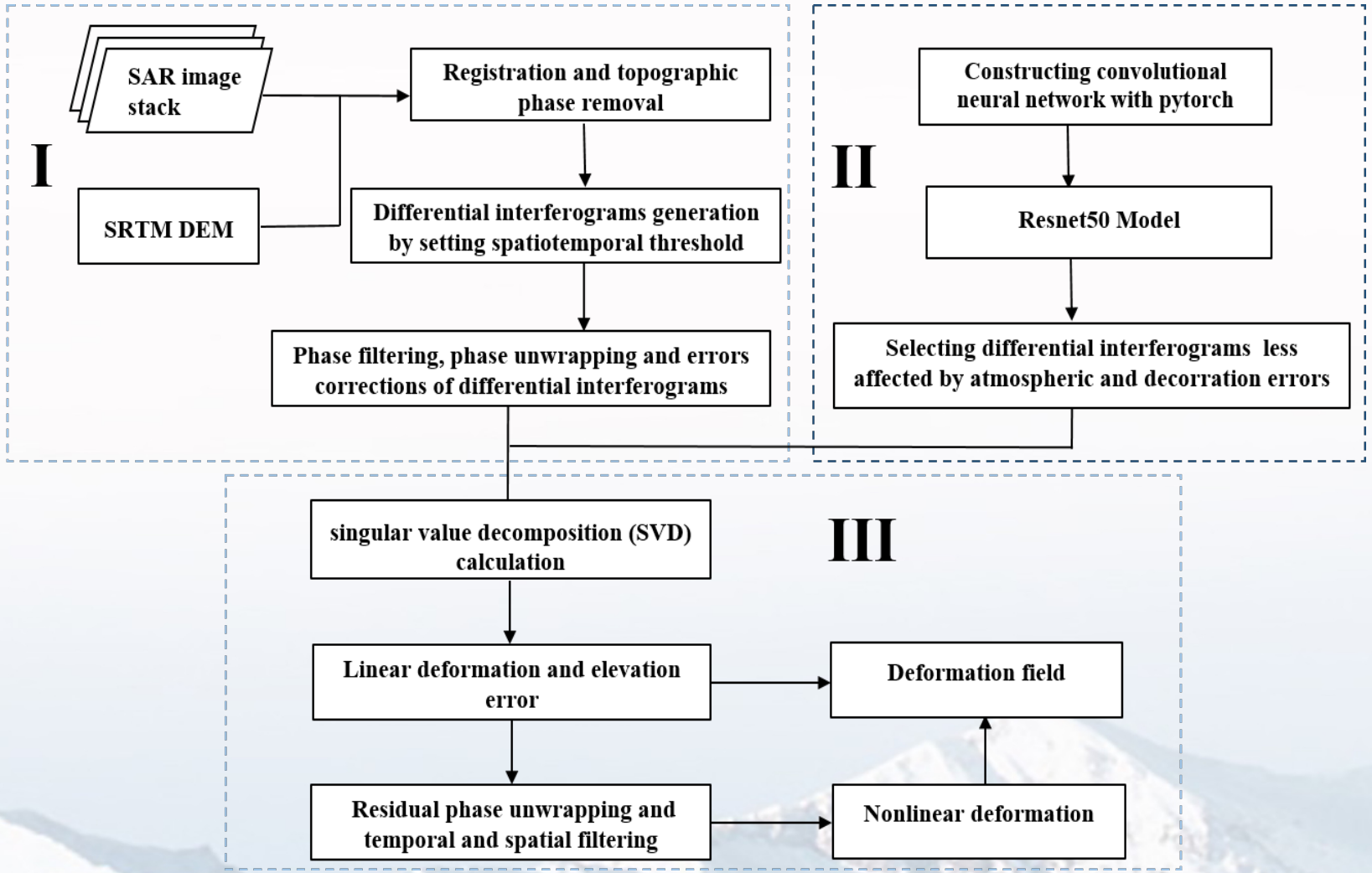

Figure 1. Workflow of the proposed method.

Three Parts

(I) The calculation of differential interferograms of sequential deformations from SAR images.

(II) The automatic extraction of high-quality interferograms by the ResNet50–DCNN model.

(III) The estimation of deformation field.

2 Methods and contents

The structural design of the ResNet50 model

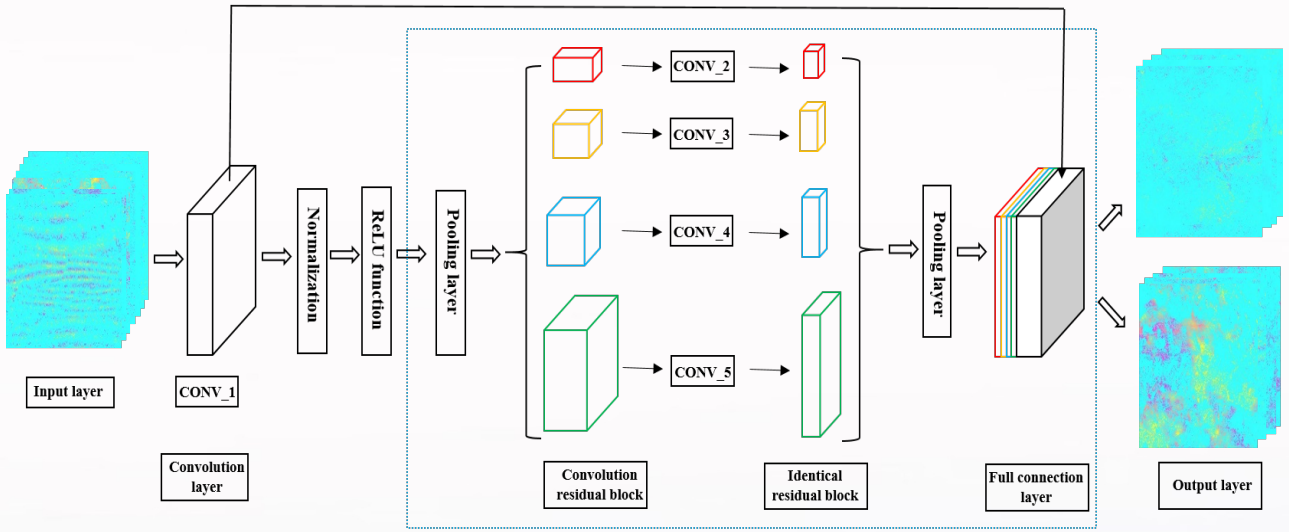

The convolution kernel sizes and output sizes of the model

Layer Name	Output Size	Configuration
CONV_1	1/2	7×7, 64, stride = 2
CONV_2	1/4	$\begin{bmatrix} 1\times1, & 64 \\ 3\times3, & 64 \\ 1\times1, & 256 \end{bmatrix} \times 3$
CONV_3	1/8	$\begin{bmatrix} 1\times1, & 128 \\ 3\times3, & 128 \\ 1\times1, & 512 \end{bmatrix} \times 4$
CONV_4	1/16	$\begin{bmatrix} 1\times1, & 256 \\ 3\times3, & 256 \\ 1\times1, & 1024 \end{bmatrix} \times 6$
CONV_5	1/32	$\begin{bmatrix} 1\times1, & 512 \\ 3\times3, & 512 \\ 1\times1, & 2048 \end{bmatrix} \times 3$
Classifier	1×1	Average pooling, Fc (Full connection), 10(Softmax

Datasets of unwrapped interferograms (Above 3000 images)

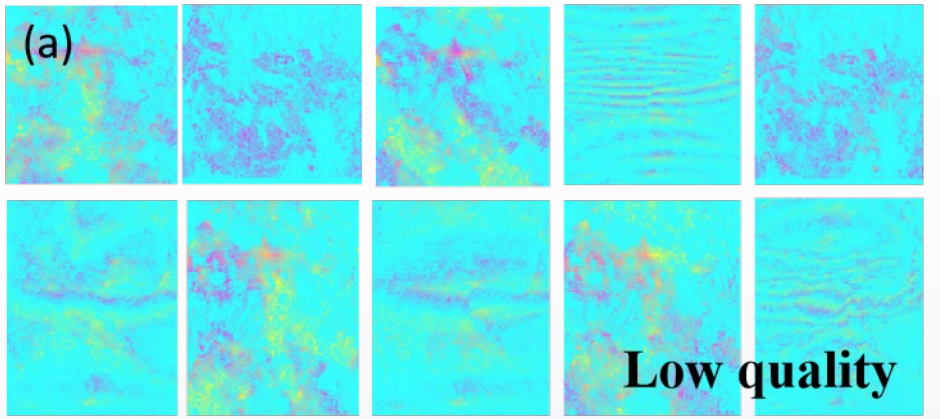

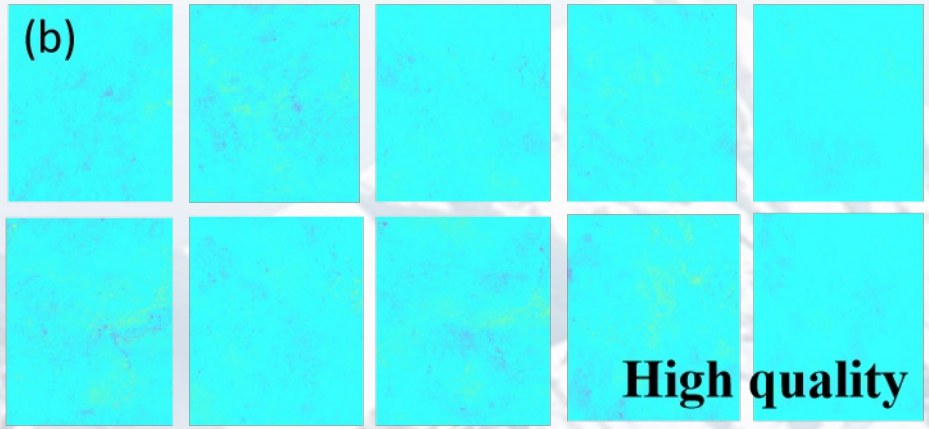

3 Experiments

3.1 Simulation Experiment

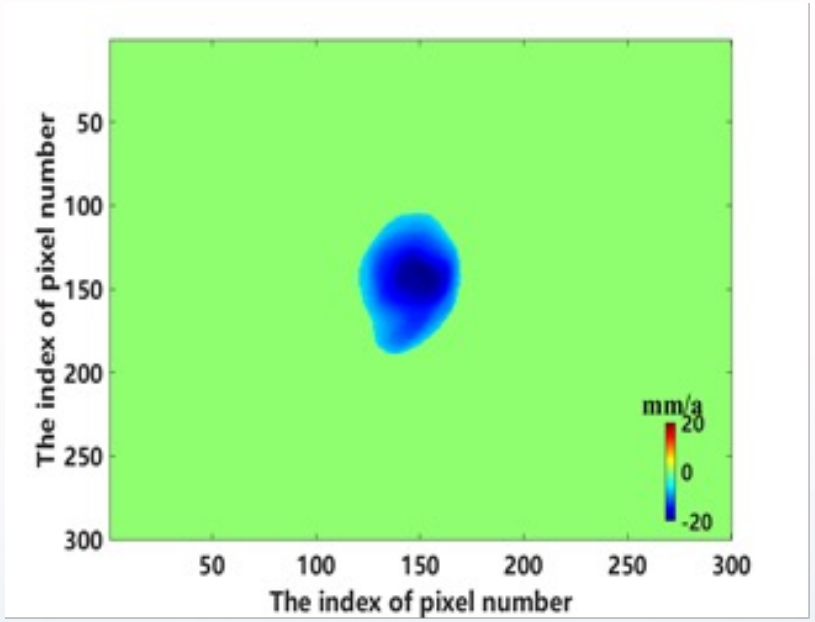

Figure2. The simulated subsidence funnel velocity with 25 mm per year

Simulated interferograms Parameters

Size of each image	The subsidence funnel velocity	Simulated interferogram number	low quality interferograms number	High quality interferograms number
300*300	**25 mm/y**	**222**	**70**	**152**

ResNet50 model Parameters

Number of training cycles	Size of input images(RGB)	Training learning rate	The activation function
200	**128 × 128**	**0.001**	**Rectified Linear Units (ReLu)**

3.1 Simulation Experiment

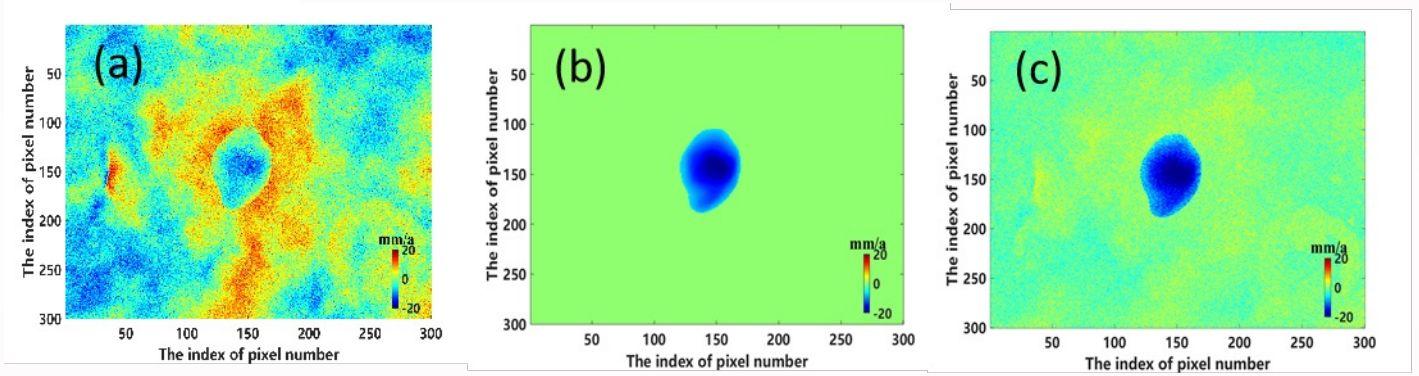

Figure3. The annual deformation rate based on (a) the spatio–temporal baseline threshold method (b) the manual method (c) the ResNet50–DCNN method.

The accuracy is above 90% for the simulation experiment .

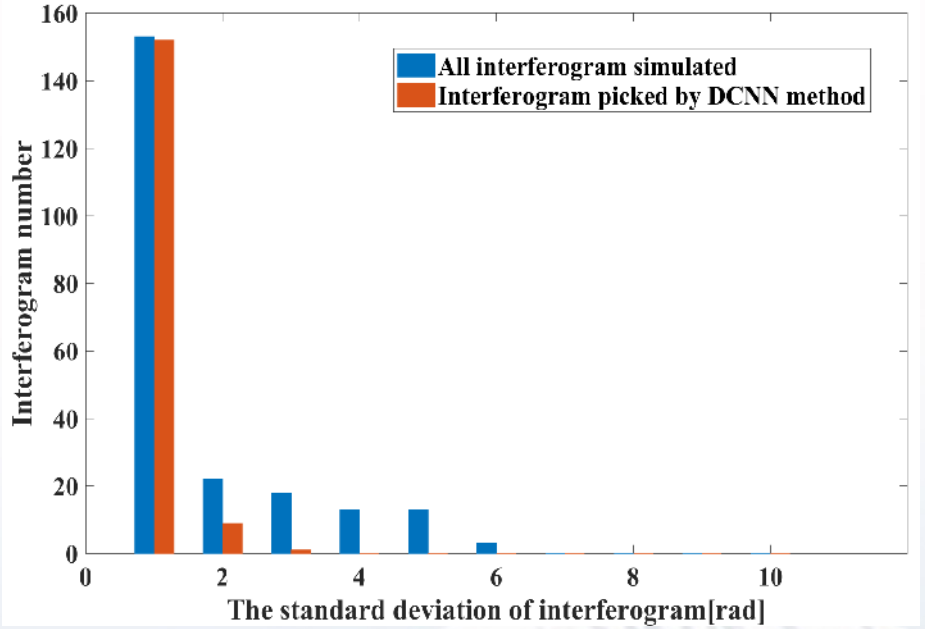

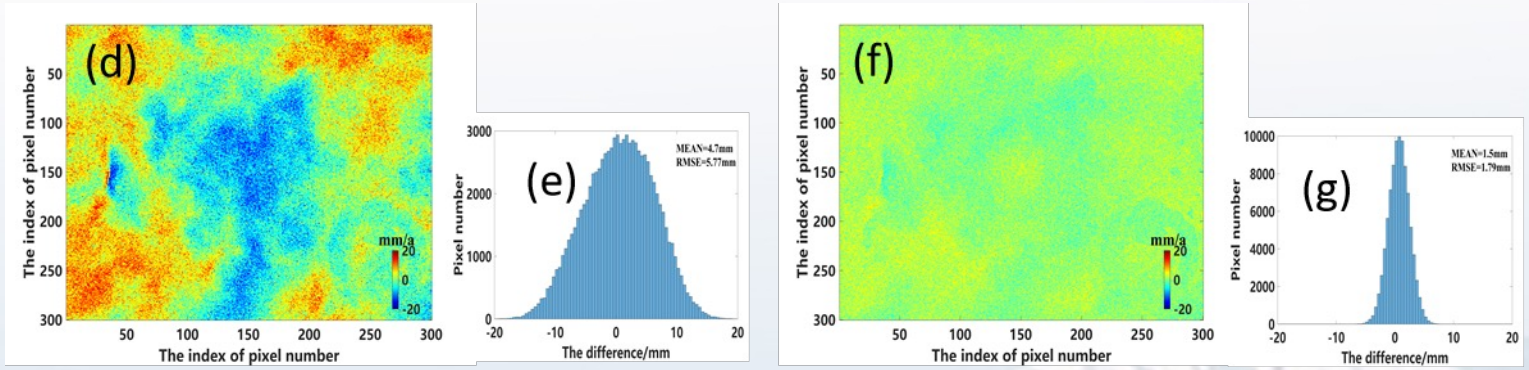

Figure4. (d) Difference between (a,b). (e) Histogram of (d). (f) Differences between (a,c). (g) Histogram of (f)

Figure5.Histogram distribution for standard deviations of the interferogram phase based on interferograms selected by the ResNet50–DCNN method and those originally simulated.

3.2 Real Experiment

Research Area and datasets

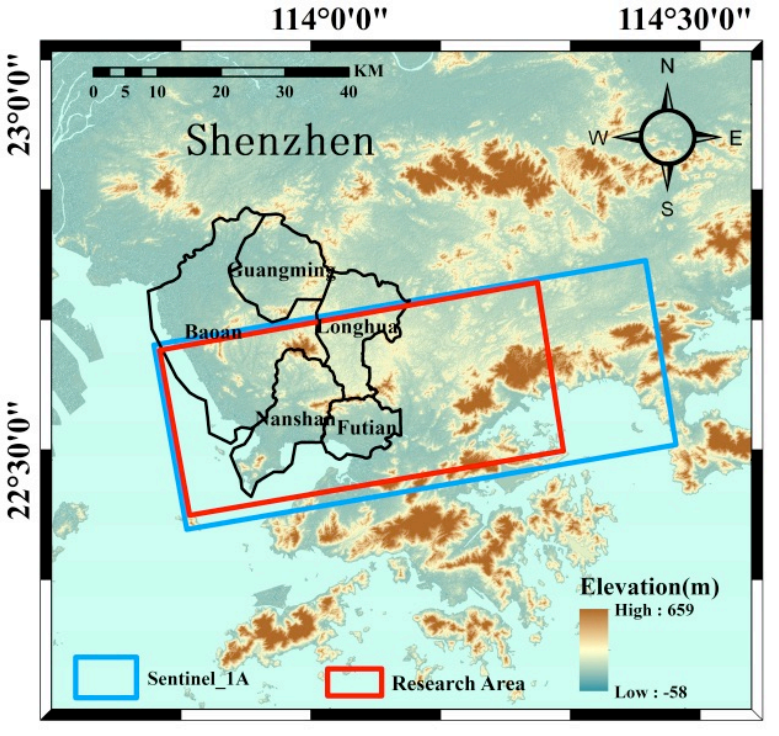

Figure 2. Overview of the research area and coverage of SAR datasets

SBAS-InSAR Parameters

Sentinel-1 images number	The time baseline threshold	The space baseline threshold	Origimal interferogram number
81	**75D**	**150m**	**593**

ResNet50 model Parameters

Number of training cycles	Size of input images(RGB)	Training learning rate	The activation function
300	**256 × 256**	**0.001**	**Rectified Linear Units (ReLu)**

3.2 Real Experiment

Results

The standard deviations of the interferograms are used to analyze the performance of the proposed method.

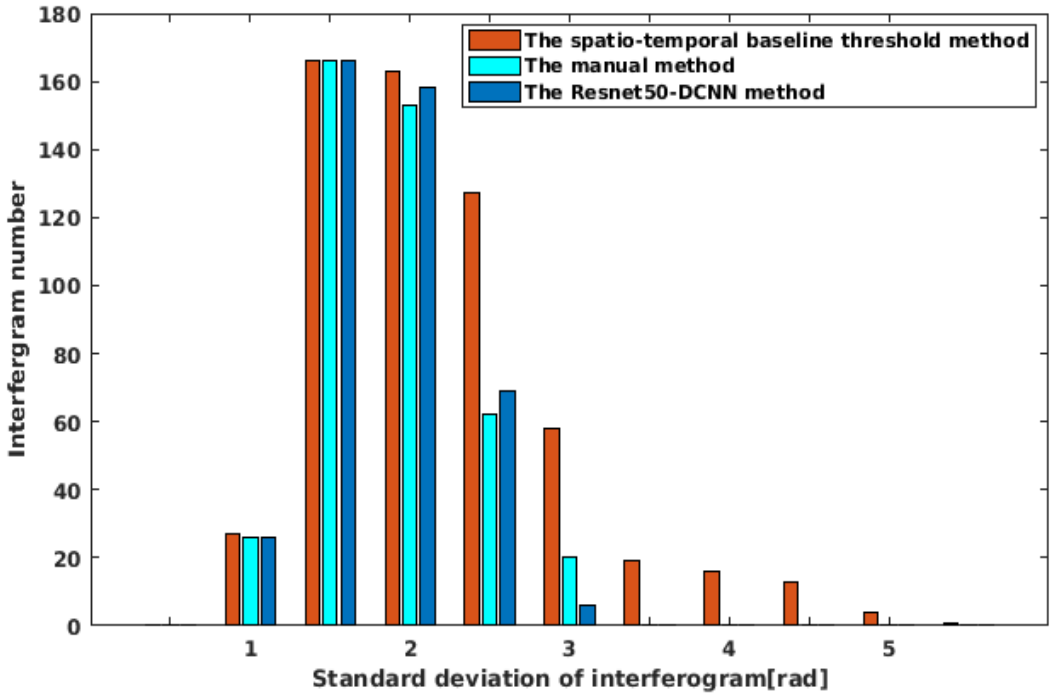

Figure 6. The distribution of the standard deviations of the interferogram phase based on the three different methods displayed in form of a histogram.

	The spatio–Temporal Baseline Threshold Method	The Manual Method	The ResNet50–DCNN Method
Number of interferogram	**593**	**411**	**425**
Standard deviation of interferogram phase/rad	**2.1054**	**1.6328**	**1.6406**

Table 1. Derived number and standard deviations of the interferogram phase obtained by the three methods.

3.2 Real Experiment

Results

The vertical deformation rates

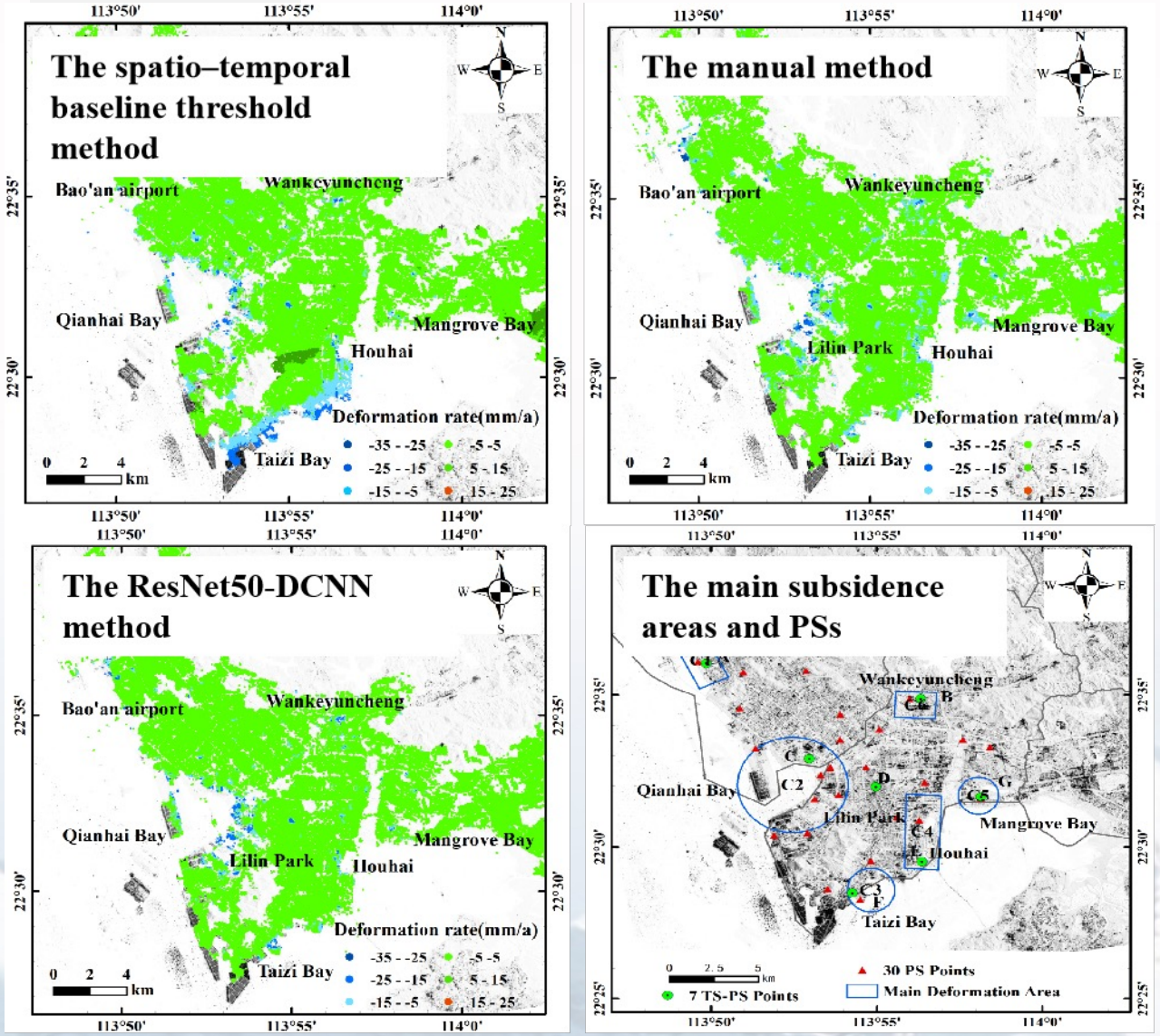

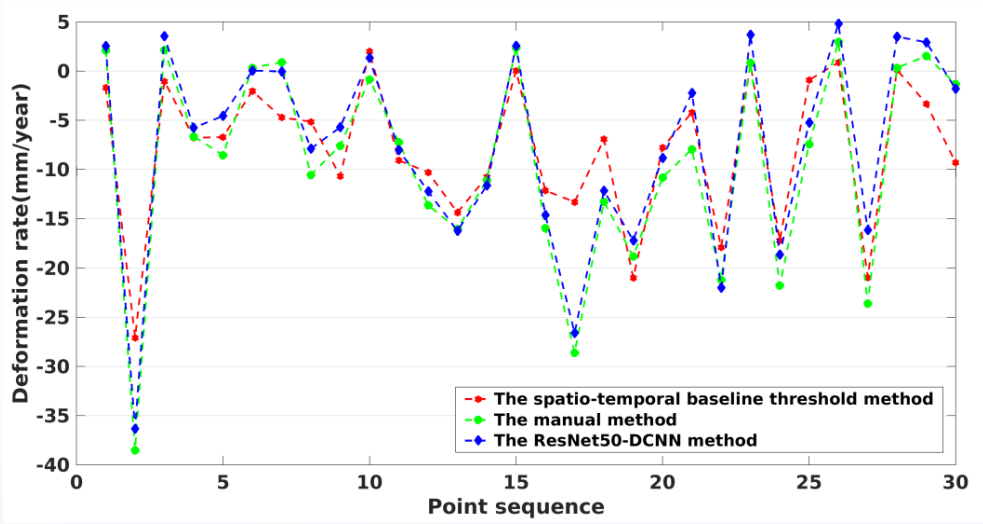

Figure 7. Annual average deformation rate of 30 randomly selected PS points obtained by the three investigated methods.

The location of subsidence areas and deformation values reflect the reliability of the proposed method.

4. Conclusion and discussion

- The quantity of high quality interferograms extracted by the ResNet50–DCNN method is **above 90% for the simulation experiment and above 87% concerning the real data experiment**, which reflects the accuracy and reliability of the proposed method.
- A comparison of the overall surface subsidence rates and the deformation information of **local PS points reveals little difference** between the land subsidence rates obtained by the ResNet50–DCNN method and the actual simulations or the manual method.

- The proposed advanced method **provides an automatized and fast interferogram selection process** for high quality data, which contributes significantly to the application of SBAS-InSAR engineering.
- For future research, we will expand the training samples and study DCNN models to further improve the general accuracy for a wider applicability of this method.

He, Y., Zhang, G., Kaufmann, H., Xu, G. Automatic Interferogram Selection for SBAS-InSAR Based on Deep Convolutional Neural Networks[J]. Remote Sensing, 2021, 13 (21): 4468。

GFZ Helmholtz-Zentrum Potsdam

EGU General Assembly 2022

哈爾濱工業大學(深圳) HARBIN INSTITUTE OF TECHNOLOGY, SHENZHEN

Thank you!

Yufang He

[1]Navigation and Remote Sensing Laboratory, Harbin Institute of Technology (Shenzhen), Shenzhen, China

[2]GFZ German Research Centre for Geosciences, Department of Geodesy, Section of Remote Sensing, 14473 Potsdam,Germany.

Email: heyufang@gfz-potsdam.de

NH6.1 – Remote sensing big data analysis and applications in geosciences